IOP Conference Series: Materials Science and Engineering

PAPER • OPEN ACCESS

Effect of travelling magnetic field inductor characteristics on the liquid metal flow in a rectangular cell

To cite this article: E. Shvydkiy *et al* 2018 *IOP Conf. Ser.: Mater. Sci. Eng.* **424** 012012

IOP Conf. Series: Materials Science and Engineering **424** (2018) 012012 doi:10.1088/1757-899X/424/1/012012

Effect of travelling magnetic field inductor characteristics on the liquid metal flow in a rectangular cell

E. Shvydkiy[1*], I. Kolesnichenko[2], R. Khalilov[2], A. Pavlinov[2] and G. Losev[2]

[1] Ural Federal University, Mira St. 19, Yekaterinburg, Russia
[2] ICMM UB RAS, 1 Akad. Korolev St., Perm, Russia

*Corresponding author: e.l.shvydky@urfu.ru, kiv@icmm.ru, losev.g@icmm.ru

Abstract
Contactless liquid metal stirring by traveling magnetic field (TMF) inductor is widely applied in modern metallurgy. The quality of stirring is an actual challenge. One solution to this problem is to complicate the TMF inductor supplying current form. In present work we study the influence of the current on the hydrodynamic characteristics of the flow. The spatial distribution of the velocity field is investigated. The goal is to reduce stagnation zones in the flow and to achieve uniform stirring. Local turbulence characteristics, which has a significant effect on the stirring process, are also investigated. In this case, the purpose is to generate the flow with a sufficient intensity of the turbulence. The research is carried out by mathematical simulation and experiments. Three-dimensional calculations are performed in the Comsol Multyphysics software. The experiment is carried out on gallium eutectic. The total electromagnetic force dependencies on the supplying current characteristics are obtained taking into account the magnetic saturation. Three-dimensional flow calculations are verified on the experimental data. The flow characteristics on the TMF inductor supplying current value are determined.

Key words: electromagnetic stirring, travelling magnetic field, ultrasonic velocimeter, numerical analysis

Introduction

Electromagnetic processing of liquid metals has great potential. For example, at the stage of preparation of non-ferrous and ferrous metals, the use of magnetohydrodynamic (MHD) agitators significantly increases the energy efficiency of operations [1]. Electromagnetic stirring by rotating and travelling magnetic fields of crystallizing metals is one of the alternative ways to improve the quality of the material. In this connection, research aimed at increasing the efficiency of electromagnetic stirring by TMF can lead to a significant economic effect.

A number of both theoretical and experimental studies were devoted to electromagnetic mixing and presented the analytical dependencies of the fluid flow rate and mixing efficiency on the parameters of TMF [2 - 5]. However, many questions remain open, such as the effect of the transverse longitudinal end effect of a linear induction machine (LIM), as well as the depth of penetration of the magnetic field into the metal. Additional studies can give a more complete picture, define dependencies and give recommendations for electromagnetic stirring by a TMF. To carry out these studies, an experimental setup was built.

Experimental setup

The experimental setup consists of a vertical cell *1*, which is made from plexiglass. The cell is field with liquid alloy GaSnZn. The cell has dimensions 450×20×75 mm^3. The channel is placed on a linear inductor motor *2* of the TMF with dimensions of 480×350 mm^2. The TMF is created by the six coils (170 turns in one coil). The coils are powered by a three-phase programmable current source *3* Pasific Smart Source 360 ASX-UPC3. This power supply allows to specify the shape of the output signal and to modulate the TMF. The frequency of supplied current is 50 Hz. The measurements of the velocity of the flows in liquid metal phase are made by means of ultrasonic Doppler velocimeter *4* (UDV) DOP 2000, Signal Processing [6]. The four sensors *5* of the UDV are placed on the thin wall of the cell. Ultrasound Doppler velocimetry includes emitting ultrasound wave packages by an ultrasound Doppler sensor, their consequent adoption, and calculation of the Doppler frequency shift between the emitted and received wave packages. The ultrasonic silicon gel has to be used to provide sound contact between the probe and the wall. However, the presence of sound-reflecting particles moved by the flow in the medium is necessary. The gallium oxide particles reflect ultrasound waves in gallium eutectic. These particles are formed by oxidation of gallium in the atmosphere [7].

Measurements of the Lorenz force produced by the TMF inductor were carried out on a model installation. As a working medium, a copper plate measuring 589×15×288 mm^3 was used. The plate was suspended on inextensible threads, so that it could freely move over the inductor at a constant value of the air gap. Measurements of traction and lifting components of electromagnetic force were carried out using spring dynamometers. To measure the vertical component of the force, four dynamometers were placed between the pieces of hanging threads. A dynamometer measuring the planar component of the force was rigidly attached to the plate and stand frame. When the inductor is turned on, the TMF generated force displaced the plate and reduced its weight. The accuracy of the measurement of the planar force component was 0.1 N, the lifting component was 1.0 N.

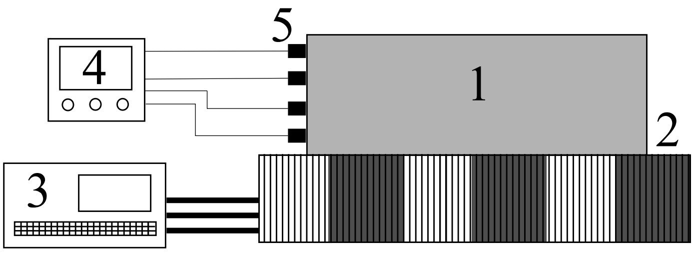

Fig. 1: Sketch of the experimental setup: 1 - channel filled with liquid metal, 2 - TMF inductor, 3 - power supply, 4 - UDV, 5 - ultrasonic sensors.

Mathematical model

3D Numerical calculations were performed by means of finite element method in Comsol Multiphysics softwere. At the first stage an electromagnetic calculation was made, based on the Maxwell equations. Considering the low magnetic Reynolds number, the induced current density was calculated Reynolds noninductive formulation [6, 8]:

$$\vec{J} = \sigma\vec{E} \tag{1}$$

where $\vec{J}$ - current density, σ - electric conductivity, $\vec{E}$ - electric field strength.
The electromagnetic force acting on a liquid metal was calculated as:

$$\vec{F}_{EM} = \vec{J} \times \vec{B} \tag{2}$$

where $\vec{B}$ - magnetic flux density.
The problem was solved in the frequency domain study for a frequency of 50 Hz. The mesh for electromagnetic part consist from 536784 tetrahedral elements. The melt lower surface was reduced due to the skin effect. Then the resulting distribution of the electromagnetic force was transferred to the hydrodynamic (HD) part as a source term of the Navier-Stokes equation:

$$\begin{gathered}\rho\frac{\partial \vec{u}}{\partial t} + \rho(\vec{u}\cdot\nabla)\vec{u} = \nabla\cdot\left[-p2\vec{I} + (\mu+\mu_T)(\nabla\vec{u} + (\nabla\vec{u})^T)\right] + \vec{F}_{EM} \\ \rho\nabla\cdot\vec{u} = 0\end{gathered} \tag{3}$$

where, ρ density; $\vec{u}$ − velocity; ∇ − nabla operator; p − pressure; μ − dynamic viscosity; $\vec{I}$ − unit matrix; μ_T − turbulent viscosity.
Calculations of the liquid metal flows were carried out using the k-ω SST RANS model. The mesh for HD calculation consists of 76554 Hexahedral uniform elements with element size 2,4 mm.

Results

The magnetic induction generated by the TMF inductor is the most important quantity. Figure 1 shows the magnetic induction curve. As can be seen, the curve is not uniform, this is due to the presence of a tooth-slot zone. The peak located in the middle of the curve can be explained by the asymmetric distribution of currents in the coils of the TMF inductor due to the longitudinal end effect. Figure 2 shows the dependence of the x and y integral Lorentz forces components on the coil current. The force is grow with increasing current as expected.
The mean velocity profile of liquid metal is shown in Fig. 3. The discrepancies between the curves obtained with the help of UDV sensors and numerical calculations lie within the permissible limits and can be explained by the assumption that the free surface is not taken into account.
The result of the numerical calculation of the velocity field under the TMF influence is shown in Fig. 5. The flow forms one main vortex, the velocity value in the lower part is greater due to the inductor proximity and the skin effect

presence. It is worth noting that this flow pattern corresponds to the one described analytically in [2].

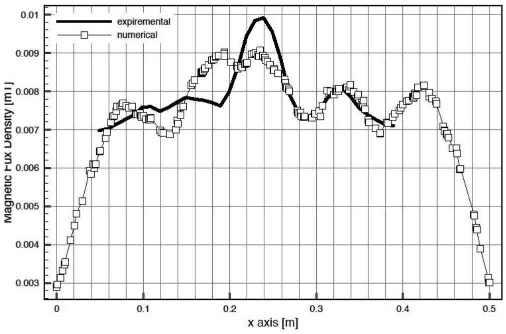

Fig. 2: Magnetic flux density on 20 mm height above TMF inductor surface

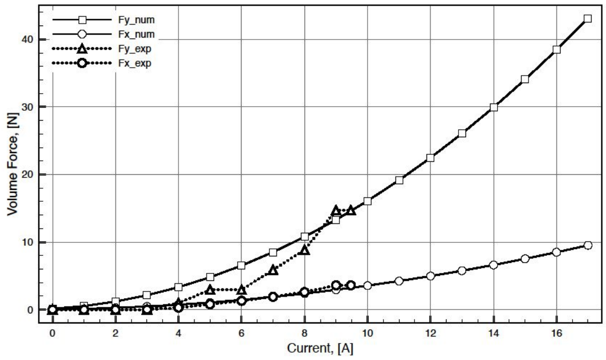

Fig. 3: Volume force verification

With an increase of magnetic flux (the supply current), the average flow velocity and hence the kinetic energy varies in different ways in different parts of the vessel (figure 6). In the first quarter, where the incoming flow creates a large-scale vortex, the average velocity is relatively weakly dependent on the magnitude of the field. In the vessel central part, the mean flow velocity dependence on the TMF is close to linear. At the vessel rear part, the average velocity reaches saturation at currents greater than 5A. Apparently, this is due to the scattering of the energy of the return flow by viscous forces.

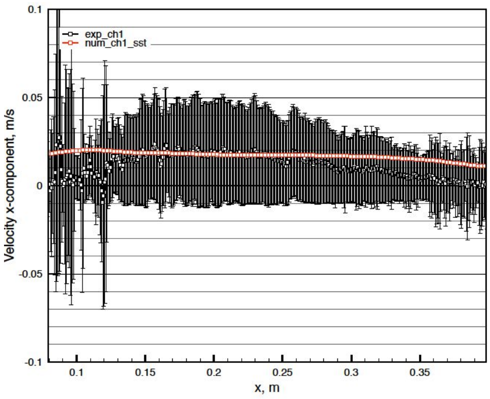

Fig. 4: Mean velocity x-component. UDV and numerical results comparison

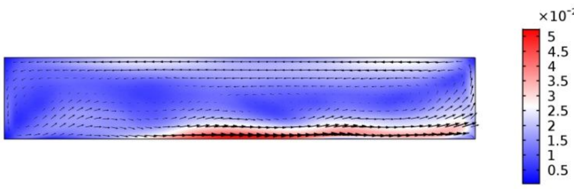

Fig. 5: Time average liquid metal flow pattern under TMF

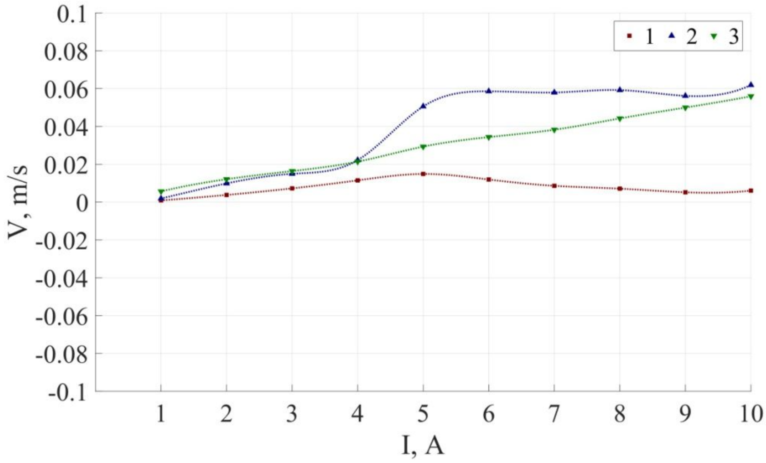

Fig. 6: Mean velocity on coil current. 1 – first quarter, 2 – second quarter and 1 – third quarter of liquid metal volume

Conclusion

An experimental setup for the study of electromagnetic mixing of TMF has been created. Experimental measurements of the magnetic field, Lorentz forces, and the flow rate of liquid metal have been carried out. A numerical model was developed and verified. Experimental and numerical experiments have shown that the flow is unsteady. Further work will be devoted to the study of flow parameters and turbulence properties under the action of a modulated magnetic field, as well as crystallization.

Acknowledgment

This work is supporting by the RFBR grant 17-48-590539_r_a.

References

1. R.B. Fdhila et al., ABB Review, 3 (2016), 45-48
2. X. Wang et al., Metall. Mater. Trans. B, 40 (2009), 104–113
3. L. Hachani et al., International Journal of Heat and Mass Transfer, 85 (2015),438–454
4. A. Kappen et al., Magnetohydrodynamics, 53 (2017), 583–593
5. M.H. Avnaim et al., International Journal of Heat and Fluid Flow, 69 (2018), 23–32
6. I. Kolesnichenko et al., Magnetohydrodynamics, 48 (2012) 221-233
7. M. Nowak, Exp. In fluids. 31 (2002), 249−255.
8. S. Denisov et al., Magnetohydrodynamics, 50 (2014) 249-265